A FUSE Survey of Supernova Remnants in the Magellanic Clouds

W. P. Blair, P. Ghavamian, R. Sankrit (JHU), & C. W. Danforth (UCol)

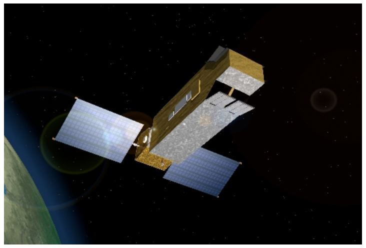

Summary: We report the progress to date from an ongoing unbiased ultraviolet survey of supernova remnants in the Magellanic Clouds using the Far Ultraviolet Spectroscopic Explorer (FUSE) satellite. Earlier work with FUSE has indicated that optical and/or X-ray characteristics of supernova remnants (SNRs) are not good predictors of the objects that will be bright in the ultraviolet. We obtained spectra of as complete a sample of Magellanic Cloud SNRs as was possible within the constraints of a FUSE survey program. We proposed 39 objects in the Large Magellanic Cloud and 11 objects from the Small Magellanic Cloud, with a standard request of 10 ks per object using the FUSE 30" square aperture. Actual observations were both higher and lower than this standard request (see Table 2). The objects cover a broad range of radio, X-ray and optical properties. To date, 39 objects have been observed in the survey and C III 977 or O VI 1032 emission have been detected in 15 of them. Thus, our survey has more than tripled the number of UV-detected SNRs in the Magellanic Clouds (from 7 to 22). We compare the optical, X-ray and UV properties of the entire sample to search for systematic trends that may shed light on the relationship among the emission in these different wavebands. We also highlight the UV characteristics of selected objects.

This work is supported by NASA grants NNG04GD15G and NNG05GD75G, both to the Johns Hopkins University.

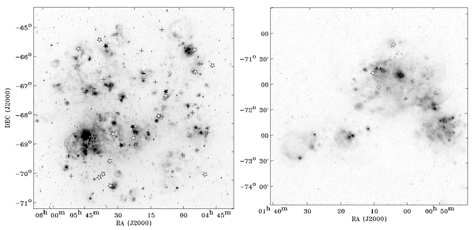

Overview H-alpha images of each Magellanic Cloud showing the spatial distribution of SNRs, using data from the SHASSA survey (Gaustad et al. 2001, PASP, 113, 1326). Filled stars are previous detections (Table 1), open stars are new detections, and non-detections are crosses. Diamonds in SMC figure (right) are pending.

Table 1. Previous *FUSE* Observations of Magellanic Cloud SNRs

Object	RA(J2000)	Dec(J2000)	ProgID	Detection?	Reference
SNR0057-7226	00:59:26.6	−72:10:05	P103,P203	Yes	1
SNR0102-7219	01:04:04	−72:01:50	A075,C083	Yes	2
SNR0505-679 (DEML71)	05:05:43	−67:52:38	P214,C072	Yes	3
SNR0509-675	05:09:32	−67:31:17	P214	No	3
SNR0519-690	05:19:34	−69:02:10	P214	Yes	3
SNR0525-696 (N132D)	05:25:01	−69:38:34	A075,B095	Yes	4
SNR0525-661 (N49)	05:26:04	−66:05:18	X005,C055	Yes	5,6
SNR0548-704	05:47:50	−70:24:52	P214	No	3

References: (1) Danforth et al. (2003); (2) Sasaki et al. (2005); (3) Ghavamian et al. (2006); (4) Beasley et al. (2005); (5) Blair et al. (2000b); (6) Sankrit et al. (2004).

Table 2. Observation Log for LMC and SMC Remnants Observed with FUSE

FUSE ID	SNR ID	Optical ID[a]	α_{J2000}	δ_{J2000}	Size (″)[b]	Exp.(ks)[e]	Detected?[f]
E90001	0448−669	...	04:48:23.0	−66:58:56.0	...	15.7(3.8)	Yes
E90002	0449−693	...	04:49:40.0	−69:21:49.0	...	11.9(2.6)	No
D90401	0450−709	...	04:50:29.7	−70:50:25.7	390×281	22(9.5)	Yes
D90402	0453.1−665	(In)N4D	04:53:14.0	−66:55:10.0	245×215	18.8	No*
D90403	0453−685	...	04:53:36.9	−68:29:29.0	140×131	9.3	No*
D90404	0453−672	DEM25,N185	04:53:47.4	−69:59:15.0	360	23.0	No*
D90405	0454.5−6713	In(N9)	04:54:33.0	−67:12:50.0	170×190	18.2(8.1)	Yes
D90406	0454−665	N11L	04:54:48.5	−66:25:40.5	60×53	15.3(2.2)	Yes
D90445	0455−687	N86	04:55:42.1	−68:39:14.9	217×183	10.9	No
D90446	0500−702	N186D	04:59:54.7	−70:08:07.1	116×116	11.3	No*
D90409	0506−680	N23	05:05:55.4	−68:01:57.0	53×53	11.6(2.7)	Yes
E90003	0506−657	...	05:06:05.0	−65:41:30.0	...	12.8	No
D90410	0509−687	N103B	05:08:59.1	−68:43:34.2	23×18	22.5(6.0)	Yes
D90411	0507−685	RXJ0507-68	05:07:30.0	−68:47:00.0	12	9.9	No
D90412	0513−692	...	05:13:41.8	−69:22:53.7	225×191	5.9	No
D90447	0519−697	N120	05:18:44.2	−69:39:12.4	104×104	20.5	No*
D90448	0520−694	...	05:19:45.1	−69:25:58.7	138×104	21.5(7.2)	Yes
E90004	0521−657	...	05:21:44.0	−65:42:05.0	...	15.6	No
D90415	0523−679	N44-shell3	05:23:05.0	−67:52:30.0	180	13.0	No
D90416	0524−664	DEML175A	05:24:20.5	−66:23:39.6	180×165	8.7	No
D90418	0528−692	LHG40	05:27:39.3	−69:12:14.8	143	6.6(0)	Yes
D90417	0527−658	DEML204	05:27:57.1	−65:50:11.1	237×212	11.5(6.9)	Yes[g]
D90432	0528−672[c]	...	05:28:25.8	−67:14:42.5	675	21.8	No
E90005	0530−701	...	05:30:37.0	−70:08:40.0	...	11.9(2.8)	Yes
D90419	0532−710	N206	05:31:55.9	−71:00:14.0	178×171	16.3(4.8)	Yes
D90420	0532−675	...	05:32:23.0	−67:31:02.0	N/A	10.5	No
D90433	0532−6731[c]	LHG48	05:32:23.2	−67:31:59.8	788	14.4	No
D90421	0534−699	...	05:33:60.0	−69:54:58.6	116×108	10.9	No
D90422	0534−705	DEM238	05:34:17.4	−70:33:25.1	179×162	11.4(4.3)	Yes
D90423	0535−660	N63A	05:35:43.1	−66:02:05.9	20×20	13.4(5.0)	Yes
D90449	0536−693	Honeycomb	05:35:49.6	−69:18:16.0	120×60	19.2	No*
D90425	0536−676	DEML241, LHG60	05:36:01.5	−67:34:49.6	188	12.6	No
D90426	0536−706	DEM249	05:36:07.4	−70:38:47.1	162×129	8.3(3.1)	Yes
D90431	0536−692	LHG62	05:36:07.7	−69:11:52.6	469×375	13.4	No
D90427	0538−693	...	05:38:14.0	−69:21:36.8	169	18.4	No*
D90428	0543−689	DEM299	05:43:07.2	−68:58:52.0	292×243	10.1	No*
D90429	0547−697	DEML316A	05:47:02.0	−69:41:18.0	270×150	12.8	No
D90430	0547−697	DEML316B	05:47:00.0	−69:43:00.0	270×150	9.8	No
D90444	0104−723	IKT25[d]	01:06:18.9	−72:05:37.4	97	7.6(0)	Yes

[a]Optical IDs (DEM) from Davies, Elliot, & Meaburn (1976), (LGH) from Long, Helfand, & Grabelsky (1981), and (N) from Henize (1956).

[b]Diameters and center coordinates from SNR catalogs of Mathewson et al. (1983, 1984, 1985) when possible.

[c]Candidate SNR from optical echelle spectroscopy; X-ray and/or radio confirmation pending.

[d]SNR ID from X-ray catalogue of Inoue, Koyama, & Tanaka (1983).

[e]Total integration times for each object. For detections, the orbital night time fractions are given in parentheses. Note two objects with no orbital night time were still detectable.

[f]A "No" with an asterisk indicates those objects for which stellar contamination affects the ability to see potential faint emission.

[g]This SNR marginally detected only in C III. This is the only detection listed with C III but no O VI emission.

Table 2 (above) summarizes the FUSE observations and indicates objects that were and were not detected in the FUSE survey. Total and orbital night portions of the integration times are shown.

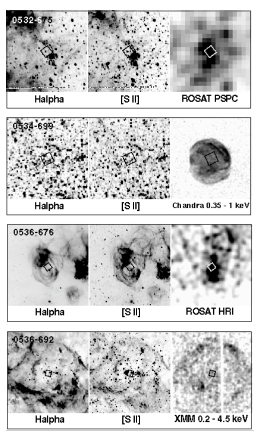

The figure above shows examples of some SNRs that went undetected by FUSE, for comparison with the imaging portions of figures above. It is not obvious from optical and X-ray appearances which SNRs will be FUV sources.

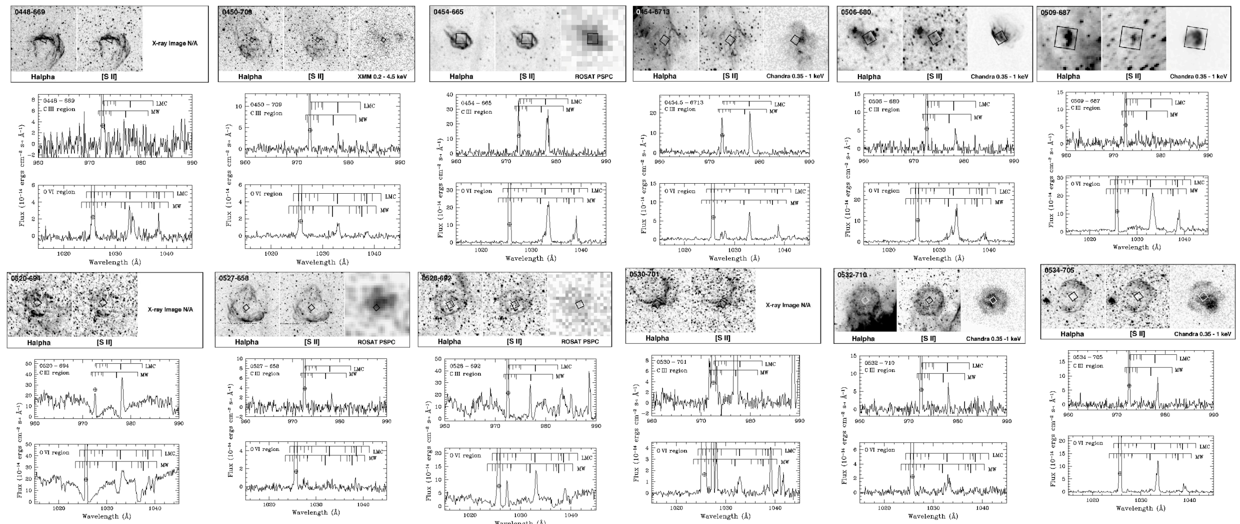

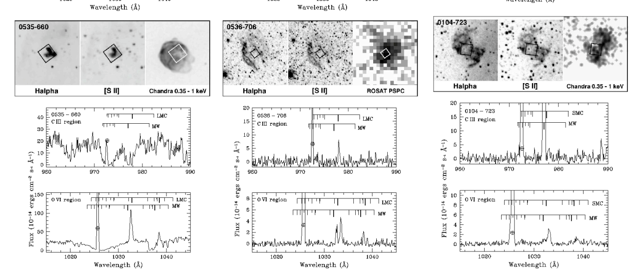

Above and right: Summary figures for FUV-detected SNRs. The top panel in each figure shows optical and X-ray images of each SNR with the FUSE LWRS aperture (30" square) overlaid for the location and position angle at the time of the observation. Top left: H-alpha; Top middle: [S II]; Top right: soft X-ray (from the source indicated by the label). The middle and bottom panels of each figure show FUSE data sections centered on C III 977, and O VI 1032,1038, respectively. Each spectral panel contains two horizontal bars with tick marks indicating the positions of potential overlying absorption features, one at zero velocity for galactic absorption (labelled MW), and one shifted to the mean velocity of the host Magellanic Cloud (+275 km/s for LMC; +165 km/s for SMC). The long, bold tick marks are at the expected positions of the C III and O VI resonance lines, which are in emission from the SNR, but potentially in absorption by overlying gas. Medium tick marks indicate positions of H_2 transitions, and short tick marks indicate positions of interstellar O I lines. Very short ticks in the bottom panel indicate the position of C II 1036.3, another very strong ISM absorption line. The earth symbols indicate terrestrial H airglow emissions from Ly-gamma (C III panel) and Ly-beta (O VI panel).

To date, our survey has already *tripled* the number of FUV-detected SN remnants in the Magellanic Clouds from 7 to 22!

Results

- Most detected SNRs show O VI and C III at relative intensities indicative of radiative shock emission at velocities in excess of 160 km/s. No obvious SN ejecta emission is present even when the FUSE aperture apparently overlaps central X-ray ejecta.
- The observed line profiles are seldom Gaussian, and the measured centroid velocities tend to be redshifted by 50 - 200 km/s from the LMC rest frame. This indicates we are typically seeing receding shell emission as it "peaks out" from under LMC halo absorption.
- Line widths are often significantly broadened above the ~100 km/s LWRS filled aperture resolution, indicating significant kinematic broadening.
- There is no simple predictor from optical or X-ray morphology as to which SNRs will be detectable in the FUV.